Numerical modeling of seismic airguns and low-pressure sources

Leighton M. Watson, Eric M. Dunham, and Shuki Ronen

ABSTRACT

There is significant interest in understanding the dynamics of seismic airguns and the coupling between the bubble produced when the airgun discharges and the pressure waves excited in the water. It is desirable to increase the low frequency content of the signal, which is beneficial for imaging, especially for sub-salt and sub-basalt exploration, and to reduce the high frequency content, which, due to attenuation and scattering, is less useful as seismic signal, yet is thought to be damaging to marine life. It has been argued that a new style of airgun, with drastically lower pressure and larger volume than conventional airguns, will achieve these improvements. We develop a numerical model of a seismic airgun and compare the simulation results to lake data for validation. We perform numerical simulations for a range of airgun firing parameters and demonstrate that the proposed low pressure source (4000 in^3, 600 psi) is able to reduce the high frequency noise by 6 dB at 150 Hz compared to a 1000 in^3 airgun at 2000 psi, while maintaining the low frequency content. Therefore, the low pressure source is more environmentally friendly without compromising survey quality.

INTRODUCTION

Seismic airguns are the predominant source used in marine seismic surveys. They function by discharging highly pressurized air forming a bubble that expands and contracts in the water, exciting pressure waves over a wide range of frequencies. These waves are used to image targets of interest. Several studies have emphasized the need for improved low frequency content (below 30 Hz) for sub-salt and sub-basalt imaging (Ziolkowski et al., 2003). The high frequency energy (above 150 Hz) is generally useless for seismic imaging as it is attenuated before it reaches the target or scattered by the heterogeneous overburden. In addition, current seismic acquisition and processing techniques sample at 2 ms and only utilize frequencies up to $\sim$220 Hz. Thus, reducing the proportion of high frequency energy generated would improve the efficiency of the airgun. Furthermore, ocean noise from marine seismic surveys is thought to have a significant impact on marine life (Weilgart, 2007; Nowacek et al., 2015). The specific impact of marine seismic surveys on the plethora of different marine species is complicated and understanding is hampered by limited data (Weilgart, 2013). However, it is likely that reducing the high frequency noise that is not used

for seismic imaging will have environmental benefits without compromising survey quality.

Chelminski et al. (2016) proposed a low-pressure source (LPS) with radically reduced pressure and increased volume. They argue that the LPS will be more efficient and have lower high frequency content, alleviating environmental concerns. To investigate this idea, Chelminski Technology and Dolphin Geophysical conducted field tests of a LPS prototype in June 2015. Due to experimental limitations, the field measurements were restricted to a limited range of airgun parameters. Furthermore, the prototype tested had a much smaller volume than that of the proposed LPS.

In this work we develop a numerical model for seismic airguns, based on the work by Ziolkowski (1970). We validate the model against data from the field tests of the LPS prototype. Previous authors (e.g., Landrø and Sollie, 1992; Li et al., 2014; de Graaf et al., 2014) have developed more complicated models and performed sophisticated inversions to find the best fitting model parameters. Here, we focus on the predictive capability of forward modeling. We perform numerical simulations to investigate airgun configurations that were not tested in the lake and to predict whether the full scale LPS will be more efficient and produce less high frequency than a conventional airgun.

DATA

Data were collected over two days at Lake Seneca, a ∼200 m deep lake in upstate New York. The LPS prototype was suspended at variable depth from a crane over the side of the boat. Two airgun volumes, 598 in^3 and 50 in^3, were tested at a range of depths (5, 7.5, 10, 15, and 25 m measured depth) and pressures (135 psi to 1320 psi for the 598 in^3 airgun and 510 psi to 1850 psi for the 50 in^3 airgun). Observations were made with a near-field hydrophone 1 m above the airgun and with a 24 channel downhole array 75 m below, with a spacing of 2 m between the channels. The near-field hydrophone recorded at a rate of 2 kHz and the far-field array recorded at 32 kHz. The far-field observations are high quality and are recorded at much higher temporal resolution than in industry seismic surveys, where 0.5 kHz is the standard sampling rate. The near-field observations are clipped at large amplitudes. Therefore, we focus on the far-field observations recorded on the first channel of the downhole array, 75 m below the airgun.

The Rayleigh-Willis equation is a well known formula used in the exploration industry to estimate the dominant frequency of a seismic airgun (Rayleigh, 1917; Willis, 1941; Cole, 1948):

$$f = k\frac{(1 + D/10)^{5/6}}{(p_a V_a)^{1/3}}, \tag{1}$$

where D is the depth of the airgun in meters, p_a and V_a are the pressure and

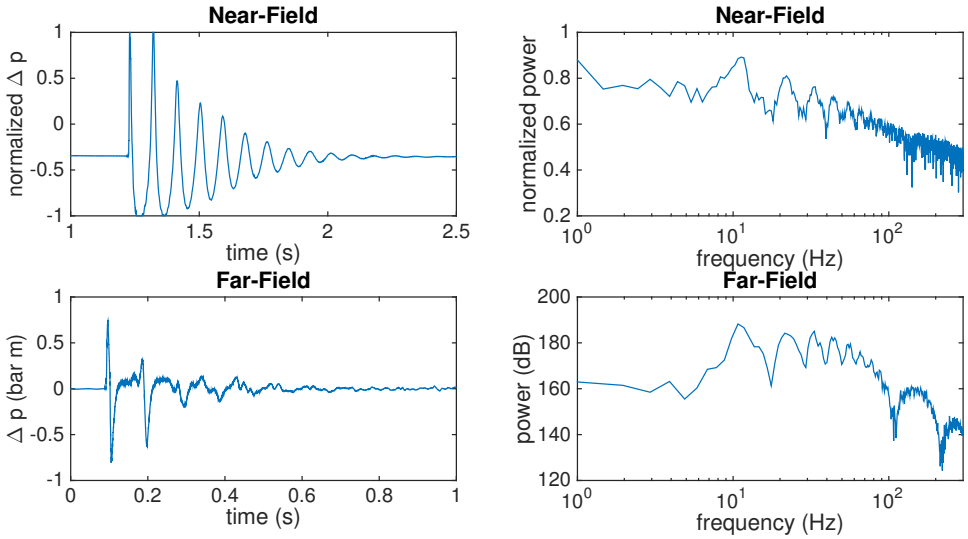

Figure 1: Example of near-field (1m from airgun) and far-field (75 m from airgun) data. The near-field measurements are clipped at large amplitudes and noisy at high frequencies. [**CR**]

volume of the airgun, respectively, and k is a constant. We are interested in how the high and low frequency components of the signal change when the airgun parameters are varied. Therefore, we need to develop a numerical model of the system that can capture all of the frequency information, rather than just the dominant frequency.

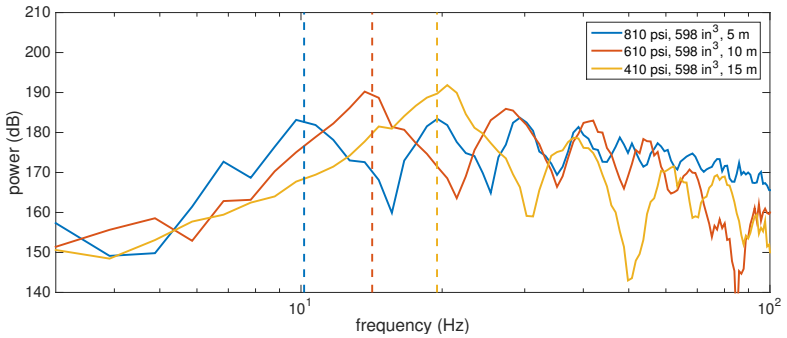

Figure 2: The Rayleigh-Willis equation (dashed) accurately predicts the dominant frequency of the far-field data (solid) across a range of different firing parameters. [**CR**]

MODEL

Since the seminal paper by Ziolkowski (1970) there has been extensive work on numerical modeling of seismic airguns (e.g., Schulze-Gattermann, 1972; Safar, 1976;

Ziolkowski, 1982; Li et al., 2010; de Graaf et al., 2014). We follow a similar treatment, assuming that the internal properties of the airgun and bubble are spatially uniform and that the bubble is approximately spherical. The first assumption poses a restriction on the temporal resolution of our model, limiting the model resolution to time scales long compared to the time it takes for a sound wave to propagate across the airgun and bubble. The resolution will vary depending upon the size and physical properties of the bubble. For the bubble at equilibrium the upper bound on the resolution is approximately 1 ms, corresponding to a frequency limit of 1 kHz. The second assumption is well satisfied as the bubble radius ($\sim$1 m) is far smaller than the wavelengths that we are interested in (>10 m). Therefore, it is appropriate to treat the bubble as a point source.

We solve the Euler equations governing the motion of a compressible fluid and evaluate the solution on the bubble wall to give a nonlinear ordinary differential equation for the bubble dynamics. Our work differs from previous studies (e.g., Ziolkowski, 1970; de Graaf et al., 2014) as we use the modified Herring equation (Herring, 1941; Cole, 1948; Vokurka, 1986) rather than the Gilmore (1952) equation to describe the bubble motions. The modified Herring equation is

$$R\ddot{R} + \frac{3}{2}\dot{R}^2 = \frac{p_b - p_\infty}{\rho_\infty} + \frac{R}{\rho_\infty c_\infty}\dot{p_b} \tag{2}$$

where R and $\dot{R} = dR/dt$ are the radius and velocity of the bubble wall, respectively, p_b is the pressure inside the bubble, and p_∞, ρ_∞ and c_∞ are the pressure, density, and speed of sound, respectively, in the water infinitely far from the bubble. Without the $\dot{p_b}$ term, equation 2 is the Rayleigh equation (Rayleigh, 1917) which is a statement of conservation of momentum for an incompressible fluid. The $\dot{p_b}$ term is a correction for compressibility that allows for energy loss through acoustic radiation. The Herring equation assumes a constant, rather than pressure dependent, speed of sound, which is well justified as $\dot{R}/c \ll 1$. The modified version of the Herring equation neglects the $(1 - \dot{R}/c_\infty)$ type correction factors (Vokurka, 1986).

The bubble is coupled to the airgun by mass conservation. We solve for the exit velocity of the flow out of the airgun at each time step rather than assuming choked flow. If the ratio of the airgun pressure to the bubble pressure, p_a/p_b, is less than a critical value, $((\gamma+1)/2)^{(\gamma/(\gamma-1))}$ then the flow is unchoked and the rate of mass transport into the bubble is

$$\frac{dm_b}{dt} = p_a A \Big(\frac{\gamma}{R_G T_a}\Big)^{\frac{1}{2}} \Big(\frac{2}{\gamma-1}\Big)^{\frac{1}{2}} \left[\Big(\frac{p_a}{p_b}\Big)^{\frac{\gamma-2}{\gamma}} - 1\right]^{\frac{1}{2}} \tag{3}$$

Otherwise, the flow is choked and the equation for the rate of mass transport reduces to

$$\frac{dm_b}{dt} = p_a A \left(\frac{\gamma}{R_G T_a} \right)^{\frac{1}{2}} \tag{4}$$

where m_b is the mass inside the bubble, A is the area of the airgun port, T_a and p_a are the temperature and pressure of the airgun, respectively. γ is the ratio of the specific heats at constant pressure and volume, 1.4 for an ideal gas. R_G is the specific gas constant for dry air, 287.06 J/kgK.

The mass inside the airgun, m_a, is evolved by mass conservation.

$$\frac{dm_a}{dt} = -\frac{dm_b}{dt} \tag{5}$$

The air inside the airgun and the bubble is treated as an ideal gas.

$$p = \frac{m R_G T}{V} \tag{6}$$

The airgun is assumed to discharge adiabatically. The temperature of the bubble is governed by the first law of thermodynamics for an open system. This allows for heat conduction across the bubble wall and accounts for the energy associated with the advection of mass from the airgun into the bubble.

$$m_b c_v \frac{dT_b}{dt} = (c_p T_a - c_v T_b) \frac{dm_b}{dt} - 4\pi M \kappa R^2 (T_b - T_\infty) - p_b 4\pi R^2 \dot{R} \tag{7}$$

The first term on the right relates to the transport of energy when mass is advected into the bubble. The second term is the heat exchange between the gas in the bubble and the surrounding water. κ is the heat transfer coefficient and M is a constant that accounts for the effect of turbulence increasing the effective area over which heat transfer can occur. The third term is the rate of work done. c_v and c_p are the specific heats at constant volume and pressure. They are 718 J/kgK and 1010 J/kgK, respectively.

Combined with the modified Herring equation, these equations give a system of nonlinear ordinary differential equations for the coupled bubble and airgun system. We solve this using an explicit Runge-Kutta (4,5) solver with variable time-stepping. Figure 3 shows example model outputs, for the airgun and the bubble.

The pressure perturbation in the water is related to the bubble dynamics by Keller and Kolodner (1956)

$$\Delta p(r,t) = \rho_\infty \left[\frac{\ddot{V}(t - r/c_\infty)}{4\pi r} - \frac{\dot{V}(t - r/c_\infty)^2}{32\pi^2 r^4} \right], \tag{8}$$

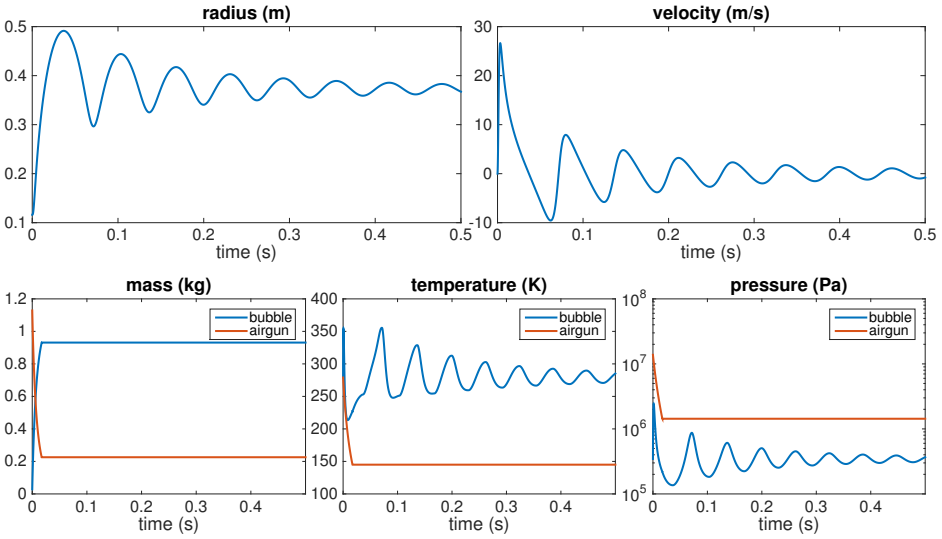

Figure 3: Example model outputs for a 400 in^3 airgun pressurized to 2000 psi disharged at a depth of 25 m. The airgun ports open at $t = 0$ and close at $\sim$0.01 s. [**CR**]

where Δp is the pressure perturbation in the water, r is the distance from the center of the bubble, and $V = \frac{4}{3}\pi R^3$ is the volume of the bubble. The second term on the right side is a near-field term that decays rapidly with distance and is negligible in the far-field. For the parameter space relevant to seismic airguns, equations (2) and (8) give identical results to the equivalent Gilmore (1952) formulations.

The observed pressure perturbation in the water is a superposition of the direct arrival and the ghost, which is a wave that is reflected from the surface of the water and arrives at the receiver at a later time. In the near-field, the amplitude of the ghost is much smaller than that of the direct arrival as the ghost travels along a much longer path, reducing the amplitude by geometrical spreading. In the far-field, the path length for the direct arrival and the ghost are almost the same. The ghost must be accounted for in order to accurately simulate the observed pressure perturbations, especially in the far-field. The pressure perturbation due to the ghost signal is calculated by replacing the path length of the direct arrival, r, with the path length of the ghost, $r + 2D$, in equation (8). The sea surface is assumed to have a reflectivity of -1 (Ziolkowski, 1982). The reflectivity can be frequency dependent, especially in rough seas. The lake surface was relatively flat during data acquisition and we found that -1 was an appropriate choice for this work.

The observed pressure perturbation, Δp_{obs}, is a superposition of the direct arrival and the ghost. For a vertically down-going direct wave, as is the case for our acquisition geometry, the observed pressure perturbation in the water is computed by

$$\Delta p_{obs}(r,t) = \Delta p_d(r,t) - \Delta p_g(r+2D,t), \tag{9}$$

where Δp_d and Δp_g are the pressure perturbations from the direct arrival and the ghost, respectively. Equation 9 assumes linearity and is only valid when the pressure perturbation is dominated by the first term in equation 8, as is the situation for the work shown here.

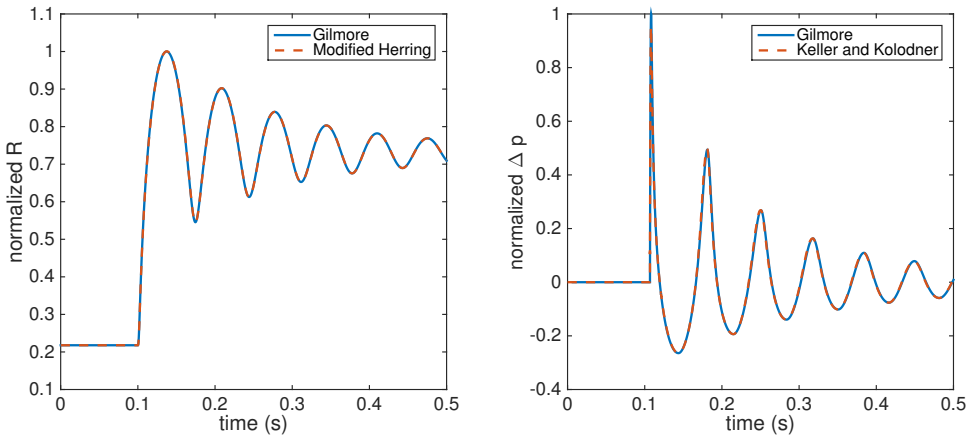

Figure 4: Bubble radius (top) and near-field pressure perturbation in the water, $\Delta p = p_b - p_\infty$, (bottom) as computed by the Gilmore (1952) equations and and with the analogous equations from Herring (1941) and Keller and Kolodner (1956), which are used in this work. The bubble radius from the modified Herring equation is used as an input to the Keller and Kolodner (1956) pressure equation. The bubble radius and pressure perturbation are normalized by the maximum of the Gilmore (1952) solutions. The initial conditions of Ziolkowski (1970) are used where the initial volume of the bubble is equal to the volume of the airgun. The discontinuity in the derivative of the radius and pressure is due to the airgun port opening instantaneously. [**CR**]

MODEL VALIDATION

In order to validate our model, we compare our simulation results to the lake data. The model has several tunable parameters. We tune these parameters so that the model fits the far-field data for one airgun firing configuration (Figure 5). We can then match the measurements from the other firing configurations by varying the airgun properties (Figure 6). This is done without any further tuning of the model parameters.

The magnitude of the pressure perturbation depends upon the location of the receiver relative to the airgun. To remove this dependency, we normalize all observations and simulations by multiplying the pressure perturbation by r, the distance from the airgun to the receiver and state the result in bar m. The port area of the airgun used in the lake was measured as 11 in^2. In our simulations, we use a reduced

area of 4 in^2 to best fit the data. de Graaf et al. (2014) used a similar approach to avoid over predicting the amplitude of the initial peak.

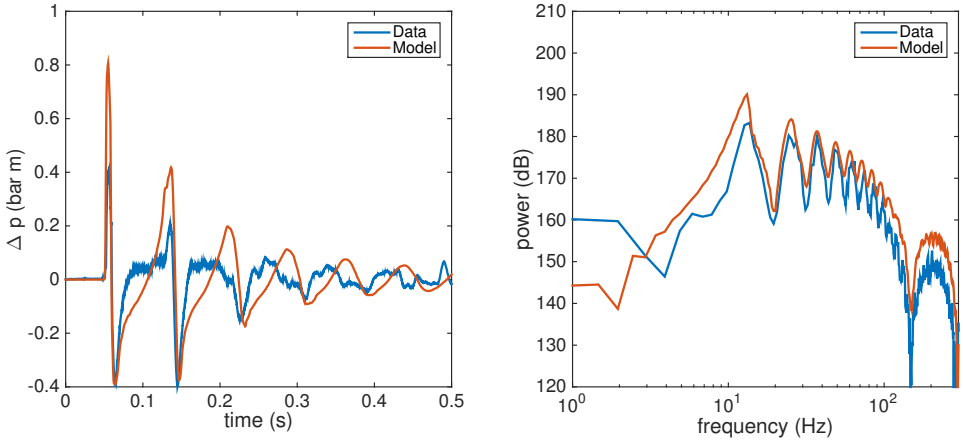

Figure 5: Comparison between the far-field observations and simulations in the time and frequency domain. Airgun properties are depth of 5 m, pressure of 410 psi, and volume of 598 in^3. The model parameters, relating to heat transfer and fraction of mass discharged from the airgun, are tuned to provide the best fit. [**CR**]

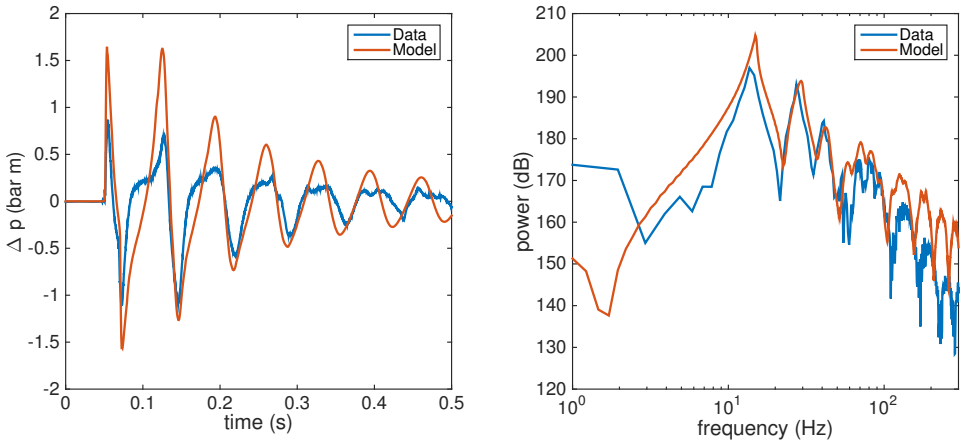

Figure 6: Comparison between far-field observations and simulations for an airgun fired at a depth of 15 m, pressure of 1030 psi, and volume of 598 in^3. The tunable model parameters are the same as for Figure 5. [**CR**]

The simulation results are in agreement with the Rayleigh-Willis equation (Figure 7) and display similar trends to the data (see Figure 2). The fit to the data and agreement with the Rayleigh-Willis equation validates our model and enables us to use it to investigate airgun firing configurations not tested in the lake, such as the proposed LPS.

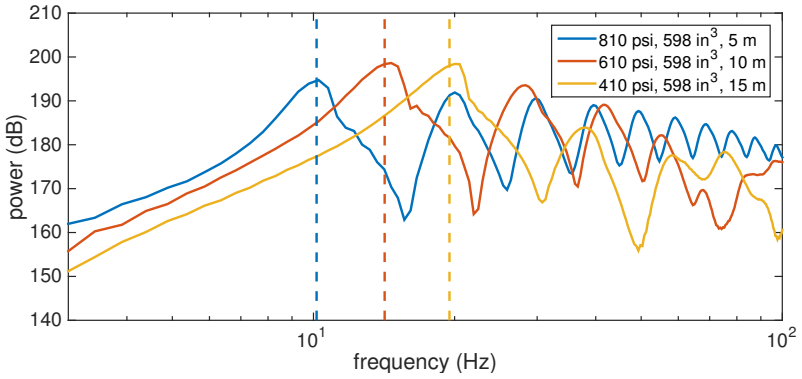

Figure 7: Simulation results are in agreement with the Rayleigh-Willis equation. The corresponding spectra for the data is shown in Figure 2. [**CR**]

LOW PRESSURE SOURCE

Conventional airguns typically have volumes of less than 1000 in^3 and are pressurized to 2000 psi. Chelminski et al. (2016) proposed a low pressure source (LPS) with a volume of up to 6000 in^3 and pressure of 600 psi to 1000 psi. The LPS will have a much larger port area than conventional airguns, 62 in^2 compared to 16 in^2.

Figure 8 shows a comparison between the simulated pressure signal for a typical conventional airgun and for the proposed LPS with the same PV value. This ensures that, according to the Rayleigh-Willis equation, they will have the same dominant frequency. The LPS reduces the high frequency noise by 5 dB at 150 Hz. This configuration is not successful at improving the low frequency content with a reduction of 1.5 dB at 3Hz from the conventional airgun. The peak-to-bubble ratio (the amplitude of the initial pressure pulse compared to the amplitude of the second pulse, which is due to the oscillation of the bubble) is reduced from 1.92 for the conventional airgun to 1.79 for the LPS. This will not degrade the quality of the data as processing can extract useful signal from the bubble as well as the initial pulse (Ronen et al., 2015).

Larger volume conventional airguns (2000 in^3) have been proposed as a solution to improve the low frequency content (Ziolkowski et al., 2003). However, the larger volume airguns are heavy and have maintenance issues because of the high pressures that they must be engineered to withstand. Therefore, they have not been widely adopted by the industry. An advantage of the LPS is that much larger volumes can be used without engineering or operational difficulties, improving the low frequency content. Figure 9 shows a comparison between a conventional airgun and a larger volume LPS (4000 in^3). The larger LPS reduces the high frequency noise by 6 dB at 150 Hz compared to the conventional airgun and has a lower dominant frequency. The low frequency content at 3 Hz is the same for the two designs. This demonstrates that increasing the volume of the LPS results in improved low frequency content, as suggested by the Rayleigh-Willis equation. Even larger volume LPS (up to 6000 in^3) can be built, and safely operated, that will generate more low frequency energy while

maintaining the environmental benefits of reduced high frequency noise.

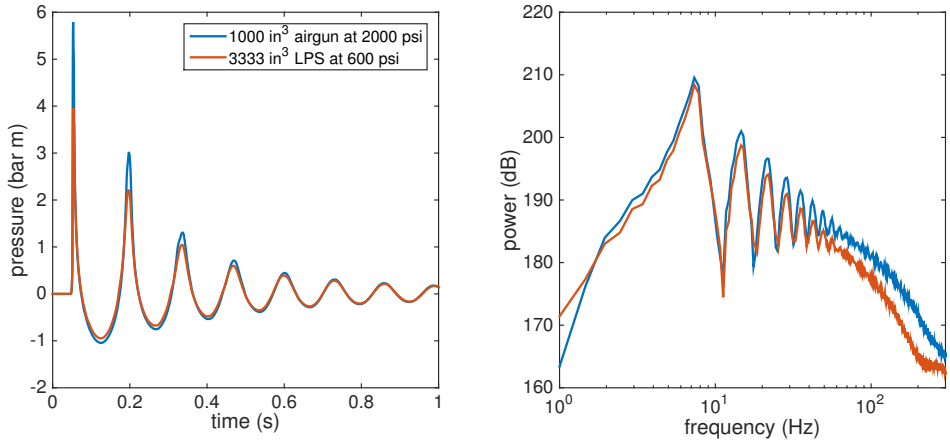

Figure 8: Comparison between simulations of the near-field ($r = 1$ m) pressure perturbation generated by a conventional airgun and a LPS fired at a depth of 7.5 m. This LPS reduces the high frequency noise but also decreases the low frequency content compared to a conventional airgun. [**CR**]

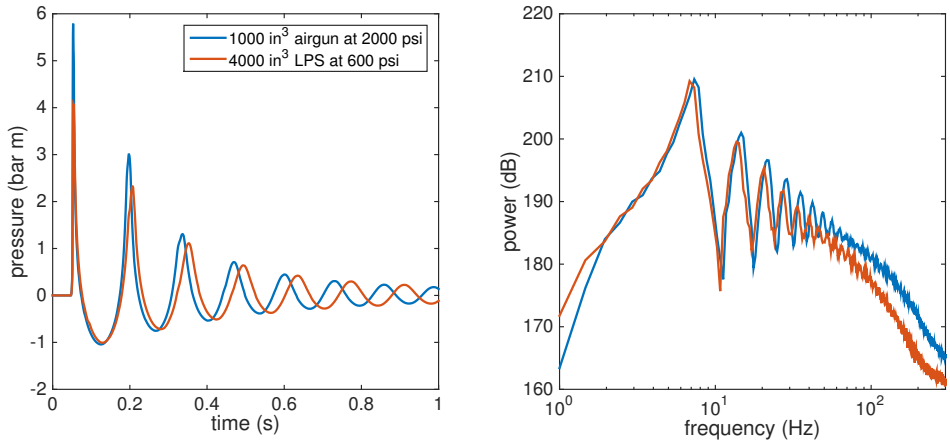

Figure 9: Comparison between simulations for a conventional airgun and a larger LPS fired at a depth of 7.5 m. The low frequency content is the same for the two designs but the LPS produces less high frequency noise. [**CR**]

CONCLUSION

There is significant interest in reducing the high frequency noise that is produced by seismic airguns as this is thought to be harmful to marine life. In addition, it is desirable to improve their imaging capabilities and efficiency. The low-pressure source has been proposed as an improvement to conventional seismic airguns that will achieve these goals.

We present a numerical model for seismic airguns and low-pressure sources that we validate against high resolution far-field data from a lake. Numerical simulations show that the proposed low pressure source can reduce the high frequency noise without compromising the usable low frequency content compared to a conventional airgun and is thus more efficient and environmentally friendly. Furthermore, the low-pressure source can be manufactured and operated at far larger volumes than conventional airguns enabling the low frequency content to be improved resulting in better sub-salt and sub-basalt imaging capabilities.

ACKNOWLEDGEMENT

We thank Chelminski Technology and Dolphin Geophysical for providing us access to the data from Lake Seneca. We acknowledge the Stanford Exploration Project and their sponsors for financial support.

REFERENCES

Chelminski, S., J. Chelminski, S. Denny, and S. Ronen, 2016, The low-pressure source: Hart's E&P Magazine, March issue, 1–4.

Cole, R. H., 1948, Underwater explosions: Princeton University Press.

de Graaf, K. L., I. Penesis, and P. A. Brandner, 2014, Modelling of seismic airgun bubble dynamics and pressure field using the Gilmore equation with additional damping factors: Ocean Engineering, **76**, 32–39.

Gilmore, F. R., 1952, The Growth or Collapse of a Spherical Bubble in a Viscous Compressible Liquid: Technical report, Hydrodynamics Laboratory, California Institute of Technology.

Herring, C., 1941, Theory of the pulsations of the gas bubble produced by an underwater explosion: Technical report, Office of Scientific Research and Development Report 236.

Keller, J. B. and I. I. Kolodner, 1956, Damping of underwater explosion bubble oscillations: Journal of Applied Physics, **27**, 1152–1161.

Landrø, M. and R. Sollie, 1992, Source signature determination by inversion: Geophysics, **57**, 1633–1640.

Li, G., Z. Liu, J. Wang, and M. Cao, 2014, Air-gun signature modelling considering the influence of mechanical structure factors: Journal of Geophysics and Engineering, **11**, 025005.

Li, G. F., M. Q. Cao, H. L. Chen, and C. Z. Ni, 2010, Modeling air gun signatures in marine seismic exploration considering multiple physical factors: Applied Geophysics, **7**, 158–165.

Nowacek, D. P., C. W. Clark, D. Mann, P. J. O. Miller, H. C. Rosenbaum, J. S. Golden, M. Jasny, J. Kraska, and B. L. Southall, 2015, Marine seismic surveys and ocean noise: Time for coordinated and prudent planning: Frontiers in Ecology and the Environment, **13**, 378–386.

Rayleigh, L., 1917, On the pressure developed in a liquid during the collapse of a spherical cavity: Philosophical Magazine Series 6, **34**, 94–98.

Ronen, S., S. Denny, R. Telling, S. Chelminski, J. Young, D. Darling, and S. Murphy, 2015, Reducing ocean noise in offshore seismic surveys using low-pressure sources and swarms of motorized unmanned surface vessels: SEG Technical Program Expanded Abstracts, 4956–4960.

Safar, M. H., 1976, The radiation of acoustic waves from an airgun: Geophysical Prospecting, **24**, 756–772.

Schulze-Gattermann, R., 1972, Physical Aspects of the Airpulser as a Seismic Energy Source: Geophysical Prospecting, **20**, 155–192.

Vokurka, K., 1986, Comparison of Rayleigh's , Herring's , and Gilmore's Models of Gas Bubbles: Acta Acustica united with Acustica, **59**, 214–219(6).

Weilgart, L., 2007, The impacts of anthropogenic ocean noise on cetaceans and implications for management: Canadian Journal of Zoology, **85**, 1091–1116.

———, 2013, A Review of the Impacts of Seismic Airgun Surveys on Marine Life: Convention on Biological Diversity Expert Workshop on Underwater Noise and its Impacts on Marine and Coastal Biodiversity, 1–9.

Willis, H. F., 1941, Underwater explosions: the time interval between successive explosions: Technical report, British Report WA-47-21.

Ziolkowski, A., 1970, A Method for Calculating the Output Pressure Waveform from an Air Gun: Geophysical Journal of the Royal Astronomical Society, **21**, 137–161.

———, 1982, An airgun model which includes heat transfer and bubble interactions: SEG Annual Meeting, Dellas, Texas, 187–189.

Ziolkowski, A., P. Hanssen, R. Gatliff, H. Jakubowicz, A. Dobson, G. Hampson, X. Y. Li, and E. Liu, 2003, Use of low frequencies for sub-basalt imaging: Geophysical Prospecting, **51**, 169–182.